ELSEVIER

Journal of Nuclear Materials 266–269 (1999) 1003–1008

journal of nuclear materials

Erosion and deposition in the ASDEX Upgrade tungsten divertor experiment

H. Maier, K. Krieger *, M. Balden, J. Roth and the ASDEX Upgrade-Team

Max-Planck-Institut für Plasmaphysik, IPP-EURATOM Association, D-85748 Garching, Germany

Abstract

Tungsten coated graphite tiles were mounted in the divertor of the ASDEX Upgrade tokamak and exposed to approximately 800 plasma discharges. After the experimental campaign, a poloidally complete set of samples was removed. The poloidal tungsten distribution pattern is presented and compared to those of other metallic impurities. The amount of tungsten detected on main chamber plasma facing components is found to be nearly unaffected by the operation of a fully tungsten covered divertor. Modifications of the tungsten surfaces are analyzed. Deposition is observed to dominate in the inner divertor while erosion prevails in the outer divertor. The influence of this result on the target plate deuterium inventories is demonstrated. Finally, a model description for the deuterium inventories observed in the main chamber is presented.

Keywords: ASDEX upgrade; Charge-exchange neutrals; Deuterium inventory; Erosion/deposition; Ion-beam analysis; Tungsten

1. Introduction

The choice of appropriate first wall materials represents a complex design task for a future fusion device like ITER [1]. It is governed by several criteria, which cannot easily be fulfilled simultaneously. The erosion behavior of a particular material affects parameters like plasma dilution and radiative cooling of the plasma as well as lifetimes of first wall components. High-Z materials in general offer the advantage of low sputtering yields compared to low-Z materials like beryllium or carbon, which would make high-Z the preferential choice from the viewpoint of component lifetime. On the other hand their ability of radiative plasma cooling is considerably higher and therefore the tolerable concentrations within the plasma are correspondingly low [2].

Another major material property is the resulting tritium retention of a fusion device. If a mix of materials for different first wall components is envisaged, this important quantity cannot be accounted for by the hydrogen retention properties of the single materials. Instead, the interplay of erosion and redeposition of various materials at various machine locations leads to a complex situation, as will be shown.

The tokamak ASDEX Upgrade was equipped with tungsten coated divertor tiles for an experimental campaign covering about 800 lower single null plasma discharges [3]. The influence of the tungsten divertor on plasma performance as well as on the impurity production and content were well diagnosed during this campaign by spectroscopic and probe measurements [4]. To investigate the long-term suitability of tungsten as a divertor target plate material, a complete poloidal set of plasma facing components was removed and analyzed after this campaign. The results of these investigations will be described in this contribution. In Section 2, the poloidal pattern of tungsten redeposition will be described. After that, results from surface analysis measurements of the tungsten coated target plates will be presented focusing on the issue of erosion and deposition. As will be shown, these results can account for the observed deuterium inventories of the divertor target plates. Finally, measurements of the main chamber deuterium inventories are presented and compared with a model description.

* Corresponding author. E-mail: ham@ipp.mpg.de.

0022-3115/99/$ – see front matter
PII: S0022-3115(98)00628-X

2. Tungsten redeposition

The amount of tungsten deposited onto the samples was determined by particle-Induced X-ray emission (PIXE) using a 1.5 MeV proton beam. Compared with Rutherford backscattering, this technique has in general a lower sensitivity but allows the unambiguous detection of tungsten even when covered by layers of low-Z material. The method has the additional advantage that it simultaneously yields information about other chemical elements. The employed setup allows the detection of characteristic X-ray lines from all elements heavier than Na. In the case of tungsten, the intensity of the L_β-doublet at 9.68/9.96 keV was employed for a quantitative analysis. This signal is nearly free from interference with characteristic lines from other chemical elements.

Fig. 1 shows the results from these measurements in a poloidal cross-section. The vertical bars denote results from samples, which were all taken from the same toroidal position, i.e. sector 10 of ASDEX Upgrade. To obtain data for the divertor region covered by tungsten, samples from the few remaining graphite tiles were analyzed. Since they served for the special purpose of target plate thermography, these tiles had not been coated with tungsten. The data points in the divertor region of Fig. 1 (i.e. regions III and IV) represent the results from these samples, which had been taken from sector 16 of ASDEX Upgrade.

As Fig. 1 shows, all main chamber components display a low and fairly constant tungsten contamination level in the range of 2×10^{15} cm^{-2}. Comparing the present data with results from samples analyzed after the previous campaign (where the failure of a tungsten covered test tile led to some contamination) [5], no significant increase can be detected. Given the accuracy of both data sets it can therefore be concluded that the amount of tungsten redeposited during the approximately 3000 s of plasma operation in the ASDEX Upgrade tungsten divertor experiment is in the range below 1×10^{15} cm^{-2}. This low value is qualitatively consistent with spectroscopic investigations, where the tungsten concentrations in the main plasma were found to be very low in general [4].

Significantly higher amounts of redeposited tungsten can be observed on the graphite tiles of the inner and outer lower divertor. The positions of maximum tungsten redeposition coincide well with the peak values of the integrated deuterium fluence for the whole experimental campaign [6]. From this observation it can be concluded that the peak values are located at the average separatrix positions which are marked in the figure by the arrows in regions III and IV. This results in a sharp maximum for the inner divertor and a broader peak for the outer divertor, because the strike point location varies for different discharge conditions on the outer target tile but remains fairly constant for the inner tile. In the case of the outer divertor the additional maximum observed in the private flux region can be ascribed to tungsten eroded at the strike point location, which is transported parallel to the magnetic field lines into the private flux zone until redeposition.

For comparison Fig. 2 shows the observed amounts of deposited iron and copper derived form the K_α line intensities of these elements. As in Fig. 1, the vertical

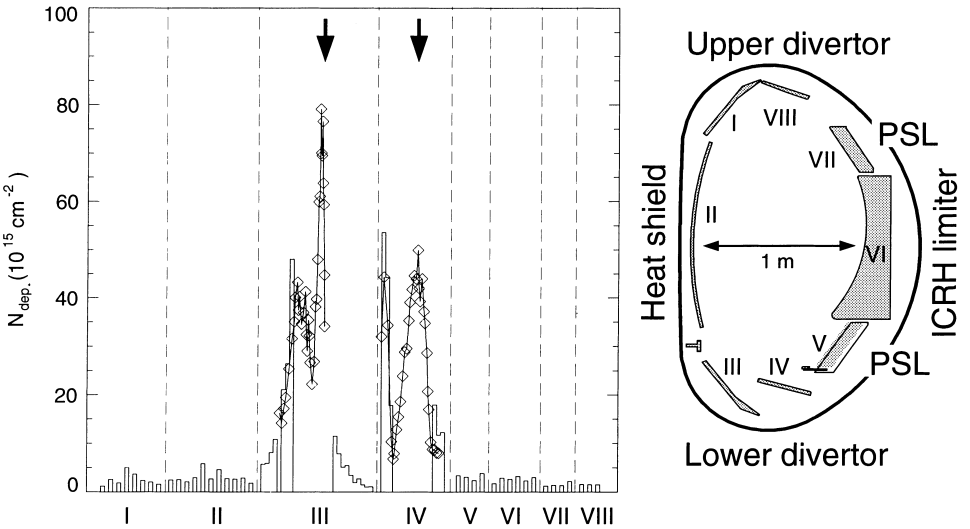

Fig. 1. Poloidal cross section of redeposited tungsten. The data are displayed according to the right-hand poloidal scheme of the ASDEX Upgrade divertor I configuration, i.e. III and IV denote the inner and outer divertor, respectively. The histogram represents data from sector 10 while the diamonds represent the results from the graphite thermography tiles of sector 16. The arrows denote the average strike point positions as determined from ion fluence measurements.

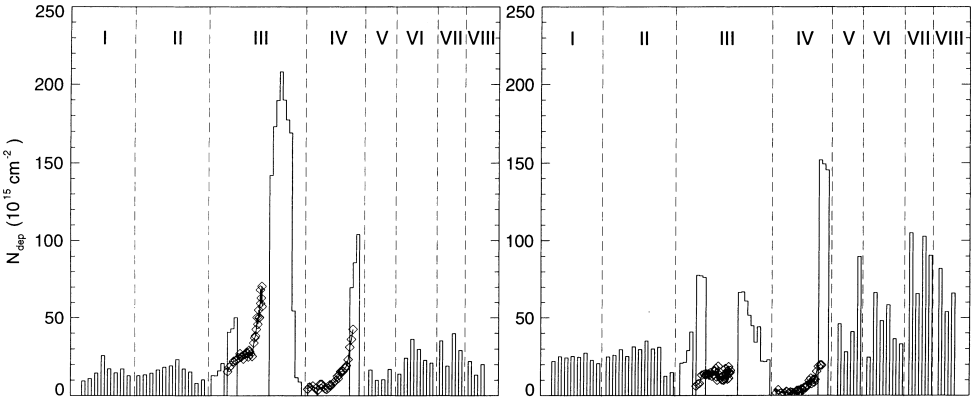

Fig. 2. Poloidal cross section of deposited iron (left) and copper (right). As in Fig. 1, the histogram represents data from sector 10 while the diamonds represent data from sector 16. For the poloidal data arrangement see Fig. 1.

bars denote the samples taken from sector 10, while the diamonds denote data taken from the thermography tiles of sector 16. A comparison of Figs. 1 and 2 demonstrates that the amounts of Fe and Cu in the main chamber are higher by more than one order of magnitude than the corresponding values for tungsten although no plasma facing components made of these materials were ever introduced in ASDEX Upgrade. Again it can be concluded that the main chamber contamination by tungsten is comparably small.

The vacuum vessel walls and various first wall support structures are steel components. The maximum value of deposited iron is found at the outboard edge of the inner divertor plate, which possibly indicates an iron source in the divertor support structure. In the case of copper the maximum amount is found on the outboard edge of the outer divertor plate. Here possible sources are the passive stabilization loop structures. The Fe and Cu data taken from the thermography tiles of sector 16 do not display a correlation with the plasma fluence, as the tungsten deposition does. In addition, the regions where the data from sector 16 and the data from sector 10 overlap poloidally, the two data sets show much larger discrepancies than in the case of tungsten. We attribute these observations to toroidally asymmetric sources for the plasma contamination by iron and copper.

3. Surface analysis of tungsten target plates

To obtain information about possible modifications of the tungsten surfaces, the target plates were analyzed with respect to their surface composition after the experimental campaign. Depth profiling of tungsten was performed by means of Rutherford backscattering (RBS) using a 2.0 MeV proton beam and the actual surface composition was determined using X-ray photoelectron spectroscopy (XPS) [6].

The XPS data revealed that apart from tungsten the surfaces were mainly composed of boron, carbon, and oxygen, respectively. On the outer target plate the composition was found to be about 12% B, 10% C, and 50% O. The high amount of oxygen is presumably due to tungsten oxide formation during storage in air. On the inner plate these percentages ranged from 10% to 30% B, 40% to 80% C, and 10% to 20% O depending on the position with respect to the geometrical shadowing [6]. The surface concentration of tungsten was found to be only 2% on the inner target tile but about 25% on the outer tile. In a simplified analysis, the RBS spectra were converted to tungsten depth profiles assuming the surfaces to be composed of a mixture of carbon and tungsten. In the following we will therefore only refer to "low-Z"-material and not distinguish the different chemical elements.

Integrating the RBS depth profiling results, total amounts of low-Z material present on the surfaces of the tungsten target plates can be determined. These are displayed in Fig. 3. Results for six locations on each, inner (top) and outer (bottom) target plate are shown. The data clearly indicate, that on the inner target plate a low-Z surface layer with a thickness of several μm had formed during the plasma exposure. On the outer plate, the surface density of low-Z material is lower by roughly a factor of five. In addition, it has to be taken into account that the tungsten covered target plates were mounted in a toroidally tilted geometry to prevent leading edges. This resulted in partial shadowing of the surfaces. Fig. 3 displays the results from the plasma wetted area of the tiles on the left-hand side and those from the shadowed area on the right-hand side. A pronounced influence of this shadowing effect on the amount of deposited low-Z material can be seen in the case of the inner target tile (top), whereas the outer tile (bottom) displays hardly any significant difference between shadowed and plasma wetted side. The shadowing effect indicates a fluence dependence of the

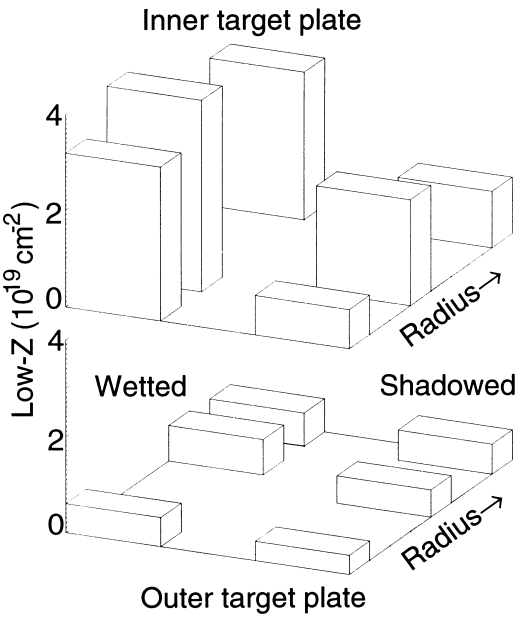

Fig. 3. Total low-Z contents for six samples of inner (top) and outer (bottom) tungsten target plate, respectively. The plasma wetted area is displayed on the left-hand side of the figure and the shadowed area on the right-hand side. The radial (poloidal) dimension of a tile is 16 cm.

thicknesses of deposited layers in the case of the inner target plate.

From these findings we conclude that the inner divertor of ASDEX Upgrade is dominated by deposition of low-Z material, while in the outer divertor erosion prevails. This conclusion can be compared with a theoretical model, where the erosion or deposition behavior of plasma exposed tungsten surfaces is predicted as a function of the plasma electron temperature and the carbon concentration in the plasma [7]. These predictions are based on numerical simulations and subsequent analytical calculations. To compare our conclusion with this model, average electron temperatures derived from Langmuir probe measurements at the target plates were determined. The results are 7.9 eV for the inner and 15.6 eV for the outer divertor. With these electron temperatures agreement between our data and the theoretical prediction can be achieved, if plasma carbon concentrations in the range of approximately 0.5–1.5% are assumed, which compare well to the about 0.5% found in the main plasma [4].

4. Deuterium inventory

4.1. Target plates

The results presented in the previous section naturally affect the balance of deuterium inventories present in ASDEX Upgrade. A detailed investigation of near-surface and total inventories found in the tungsten target plates is presented elsewhere [8–10]. Similar to the amount of deposited low-Z material, the deuterium inventory of the inner tile is about one order of magnitude higher than that of the outer tile. This indicates that the dominant mechanism of deuterium retention is co-deposition of deuterium with carbon and boron. The inventory in the outer tile is governed by implantation and diffusion into the tungsten bulk [8].

The near-surface amounts of deuterium measured by nuclear reaction analysis (NRA) using the reaction ^{3}He(d,α)p are displayed in Fig. 4. The analyzing depth with the employed incident ^{3}He energy of 790 keV is in the range of 1 μm. For these measurements eight samples had been cut out of the tiles along the plasma wetted and shadowed edge, respectively. Comparing the deposited low-Z amounts of Fig. 3 with the data from Fig. 4 for the inner target plate, it can be concluded that the deuterium concentration is larger in the shadowed area than in the plasma wetted area (0.15–0.45 D per low-Z in the shadowed region and 0.05–0.15 in the plasma wetted region). Laboratory experiments indicate that at elevated substrate temperatures the saturation concentration of hydrogen in co-deposited layers is decreased [11–13]. If we assume this to be the dominating mechanism, the data therefore indicate surface temperatures as high as 900 K [13] on the plasma wetted side of the target plate. The transient occurrence of such surface temperatures in a discharge at the end of the campaign

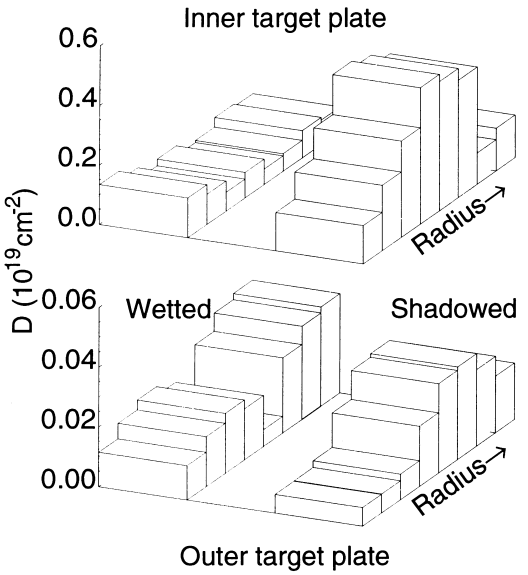

Fig. 4. Near-surface (~1 μm) deuterium amounts measured on the plasma wetted and shadowed sides of inner (top) and outer (bottom) target plate, respectively. Note the factor of 10 in the abscissa values.

would suffice to reduce the deuterium concentration accordingly.

4.2. Main chamber

Although the graphite components in the main chamber in general have experienced more plasma discharges than the tungsten covered divertor target plates (four experimetal campaigns instead of one), their deuterium inventories are lower by an order of magnitude. This observation immediately excludes the build-up of thick co-deposited layers as the main retention mechanism in the main chamber. Here we present results from a model to account for the observed inventories, which is based on the implantation of charge-exchange neutrals (CX). Details of these calculations will be published elsewhere [14].

To model such inventories, fluxes and energy distributions of CX neutrals are required for each poloidal position of ASDEX Upgrade. These have recently been obtained from B2-EIRENE computer simulations, which took experimental results at one toroidal location into account [15]. Depth distributions of implanted D in carbon have been calculated using the Monte-Carlo code TRIM.SP [16]. To integrate the deposition profile for a given CX spectrum, we parameterized these TRIM results and interpolated them using gaussian deposition profiles. Finally, the saturation level of deuterium implantation into carbon has to be taken into account. In our calculations this was done by employing the simple model of local saturation [17,18], i.e. the deuterium content in a given depth within the graphite material is taken to increase until a level of $D/C = 0.4$ is reached and kept constant from then on. Diffusion is not taken into account.

Experimental NRA data, measured as described in Section 4.1, are shown in Fig. 5 together with the results of our model. There is good agreement between experimental data (histogram) and model (solid line) on the high-field side, i.e. for the data measured on samples from the inner heat shield. On the low field side the experimental data exceed the results of the model calculation by a factor of up to five for the ICRH antenna protection limiter. We attribute these excess inventories to the fact that our modelling cannot reproduce the inventories of main chamber structures with direct plasma contact. These surfaces are subject to ion impact, both of plasma ions and impurites. Possibly diffusion due to elevated temperatures occurs and moderate co-deposition due to higher impurity fluences also cannot be ruled out. Also the employed CX spectra from B2-EIRENE do not account for the local recycling on plasma exposed limiter structures. Consequently the discrepancy is most pronounced for the ICRH antenna limiter data. To verify the model also on the low-field side of ASDEX Upgrade data from graphite surfaces without direct plasma contact are therefore needed. For this purpose NRA results from long-term samples mounted on the steel vessel walls [19] (see squares in Fig. 5) were compared with the calculated data. The experimental data represent averages from eight different toroidal positions. The resulting good agreement between model and experimental data is also displayed in Fig. 5. It can be concluded that modelling main chamber deuterium inventories for ASDEX Upgrade by implantation of charge exchange neutrals yields a good description of

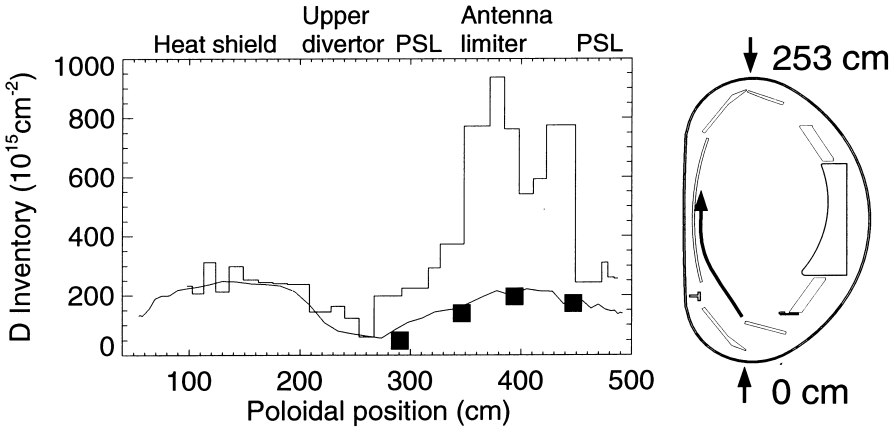

Fig. 5. Deuterium inventories in the main chamber graphite components of ASDEX Upgrade. The histogram denotes experimental data from first wall components (sector 10) as indicated above the figure, the squares are inventories measured on long-term graphite samples which had been mounted on the outer vessel wall during the tungsten campaign. They represent surfaces without direct plasma contact and are averages from eight different toroidal positions. The solid line is the result from the model described in the text calculated for fluences corresponding to 10^4 s. The poloidal position is indicated in the right-hand inset.

the experimental findings for structures without direct plasma impact.

5. Summary and conclusion

For one experimental period ASDEX Upgrade was equipped with two different first wall materials, i.e. carbon components in the main chamber and tungsten covered strike point modules in the lower divertor. This allowed the study of erosion and redeposition processes. It was found that the tungsten contamination level of all main chamber components showed no significant increase compared with results from the previous experimental campaign, where several test tiles had been installed. A comparison with the corresponding Fe and Cu data reveals that the amounts of these impurities deposited on main chamber first wall components are more than one order of magnitude higher than those of tungsten.

Surface analysis of the tungsten tiles showed that in the inner divertor region deposited low-Z material completely covered the original tungsten surface, which is a consequence of the employed material mix. This was not observed on the outer target plate. These results are in agreement with theoretical predictions, which estimate deposition of carbon to be the dominant mechanism at the electron temperatures observed in the inner divertor and erosion to dominate in the outer divertor.

The measured deuterium inventories are consequences of these observations. Since most of the low-Z plasma impurities were deposited onto the inner strike point tiles, the advantageous low permanent hydrogen retention of tungsten was outweighed by co-deposition of deuterium. For this reason the inner divertor contained more than 50% of the total deuterium inventory of ASDEX Upgrade. On the other hand, less than 10% were contained in the outer divertor.

Concerning the main chamber plasma facing components, we have presented model calculations based on the implantation of charge exchange neutrals. Comparing the results of these calculations with experimental data shows that most main chamber deuterium inventories can be accounted for by this mechanism. This implies that deposition can be neglected for such areas. The inventories of structures with direct plasma contact, such as limiters, however, are larger than the model predictions by a factor of up to five.

References

[1] R. Parker, G. Janeschitz, H.D. Pacher, D. Post, S. Chiocchino et al., J. Nucl. Mater. 241–243 (1997) 1.
[2] R. Jensen, D. Post, D. Jassby, Nucl. Sci. Eng. 65 (1978) 282.
[3] R. Neu, K. Asmussen, S. Deschka, A. Thoma, M. Bessenrodt-Weberpals et al., J. Nucl. Mater. 241–243 (1997) 678.
[4] R. Neu, K. Asmussen, K. Krieger, A. Thoma, H.-S. Bosch et al., Plasma Phys. Control. Fusion 38 (1996) A165.
[5] K. Krieger, V. Rohde, R. Schwörer, K. Asmussen, C. García-Rosales et al., J. Nucl. Mater. 241–243 (1997) 734.
[6] H. Maier, S. Kötterl, K. Krieger, R. Neu, M. Balden et al., J. Nucl. Mater. 258–263 (1998) 921.
[7] D. Naujoks, W. Eckstein, J. Nucl. Mater. 230 (1996) 93.
[8] P. Franzen, C. García-Rosales, H. Plank, V.Kh. Alimov, J. Nucl. Mater. 241–243 (1997) 1082 .
[9] D. Schleußner, P. Franzen, H. Maier, R. Behrisch, M. Balden et al., J. Nucl. Mater. these Proceedings.
[10] D. Hildebrandt, M. Akbi, B. Juettner, W. Schneider, J. Nucl. Mater. these Proceedings.
[11] A. von Keudell, W. Möller, R. Hytry, Appl. Phys. Lett. 62 (1993) 937.
[12] A. Annen, Tech. Rep. IPP 9/114, Max-Planck-Institut für Plasmaphysik, Garching (1997) .
[13] M. Balden et al., J. Nucl. Mater. these Proceedings.
[14] H. Maier et al., Deuterium inventories in first wall components of ASDEX Upgrade, Plasma Phys. Control Fusion, to be submitted.
[15] H. Verbeek, J. Stober, D.P. Coster, W. Eckstein, R. Schneider, Interaction of charge exchange neutrals with the main chamber walls of plasma machines, Nucl. Fusion, accepted for publication.
[16] M. Mayer, W. Eckstein, Nucl. Instr. Meth. B 94 (1994) 22.
[17] G. Staudenmeier, J. Roth, R. Behrisch, J. Bohdansky, W. Eckstein et al., J. Nucl. Mater. 84 (1979) 149 .
[18] S.A. Cohen, G.M. McCracken, J. Nucl. Mater. 84 (1979) 157.
[19] M. Mayer, J. Roth, unpublished data.